

OmegaCAM Secondary Standards preparatory programme - progress report

VST-TRE-OCM-23100-3356 Version 3

July 27, 2005

R. Vermeij, E.A. Valentijn & K. Kuijken

1 Introduction

The photometric calibration of OmegaCAM depends on standard star catalogs with fields that cover the complete FoV of the instrument. For the year-round calibration of the instrument, a catalog fulfilling this requirement needs to include the following standard fields: a polar field unique for OmegaCAM, and extensions of the Landolt[6] equatorial fields SA92, SA95, SA98, SA101, SA104, SA107, SA110, and SA113. These catalogs must be built for the u' , g' , r' and i' bands (known as the **key bands**).

The OmegaCAM calibration plan foresees in constructing these standard star catalogs during Commissioning and during the first year of operations using OmegaCAM itself (see req. 569, Valentijn et al. [10]). However, a preliminary first version of such a catalog is needed at Commissioning for the early verification of the presence of illumination variations (see req. 548, Valentijn et al. [10]). The initial catalog will also be used for calibrating the Exposure Time Calculator (see req. 568, Valentijn et al. [10]).

1.1 Scope of this document

For the construction of a preliminary standard star catalog, two preparatory programmes are conducted by the Consortium. These programmes are carried out with the WideField-Imager (WFI) at the ESO-2.2m, and with the INT/WFC at La Palma. The latter programme was initiated because no Sloan filters are available on WFI@ESO-2.2m. This report gives the status of these preparatory programmes.

This report was also written at the request of ESO in order to demonstrate the accuracy of the DFS pipeline. The data reduction of the photometric standards obtained from La Palma (Sect. 3) is being carried out using this software. The results thus serve as a (necessarily only partial) demonstration that the specifications of the DFS software can be met on a real dataset.

During OmegaCAM operations the task of the DFS software will be to determine a photometric zeropoint from observations of a calibrated standard star field. The La Palma and WFI programmes discussed here, on the other hand, started from a few calibration stars which needed to be propagated to the standard star fields. Thus only the scatter in the derived, individual zeropoints on a single CCD can be used as a check on the S/W at present.

The WFI data (Sect. 2) turned out to be unsuitable for establishing photometric standards, particularly because the filter set differs from the OmegaCAM set, but also because of the bad photometric conditions during the observations. The work on the WFI data has, therefore, been discontinued. The WFI data is neither used in establishing photometric standards, nor in evaluating the quality of the OmegaCAM pipeline.

Table 1: The central pointings used in the WFI@ESO-2.2m observing run.

STD FIELD	$\alpha(2000.0)$	$\delta(2000.0)$
SA 101	09 55 57	-00 23 14
SA 104	12 42 31	-00 38 36
SA 107	15 39 36	-00 12 36
SA 110	18 42 21	+00 14 52
NGC 5904	15 18 33	+02 04 58
SA113	21 40 35	+00 41 45
SA98	06 51 52	-00 19 54

2 The WFI@ESO-2.2m preparatory programme

The discussion in the following sections has been adapted from the unpublished work of Navasardyan et al. [8]. We emphasize that the WFI data set and the results derived therefrom are not used. The discussion below is added for completeness only.

2.1 Observing runs at the WFI@ESO-2.2m

Observations have been done using the WFI mosaic camera at the ESO 2.2m telescope. Observing time was allocated in three separate runs, for a total of 11 nights (April 20-26, 2000; July 9-13; February 3-7, 2001). Only 6 of these were photometric. The strategy was to cover $60 \times 60 \text{ arcmin}^2$ standard fields in the B, V, R, I broad-band filters. This required at least 4 pointings for covering the necessary field with WFI. In order to secure a wide range of magnitudes, images with both a short and a long exposure time have been taken. A fifth, central pointing with a short exposure time has also been taken of every field for cross checking the photometric accuracy. The overall covering scheme was as follows: one central and 4 lateral pointings dithered by 15 arcmin in both the RA and DEC directions. The exposure times were about 8 sec (B, V, I) and 5 sec (R) for the short exposure time images, and 2×600 sec (B), 2×250 sec (V), 2×200 sec (R) and 2×300 sec (I) for the deep images. The fields observed are given in Table 1.

For the photometric calibration of the data, we made additional observations of the PG1323 field (21 April 2000) and the Rub149 field (5 February 2001). Both fields are from the catalog of Landolt[6]. The purpose was to require a proper color baseline for the calibration equation, and a better mapping of the chip-to-chip variations of the photometric zero point.

2.2 Data reduction: pre-reduction and astrometric calibration

Only the data collected during the first and last runs have been reduced as no useful data were obtained throughout July 9-13. The priority has been given to the more covered standards fields and the fields which also contain Stetson standard stars.

Pre-reductions were carried out using the MSCRED package in IRAF. Mean combined bias and twilightflat frames have been created for each run. The WFI images observed in the I band show a very strong fringing pattern which has been removed using the average fringing pattern as provided by the ESO2.2m telescope team ¹. This average pattern has been scaled to the actual value of the fringing in the image and removed. The astrometric calibration was performed for

¹<http://www.ls.eso.org/lasilla/sciops/2p2/E2p2M/WFI/>

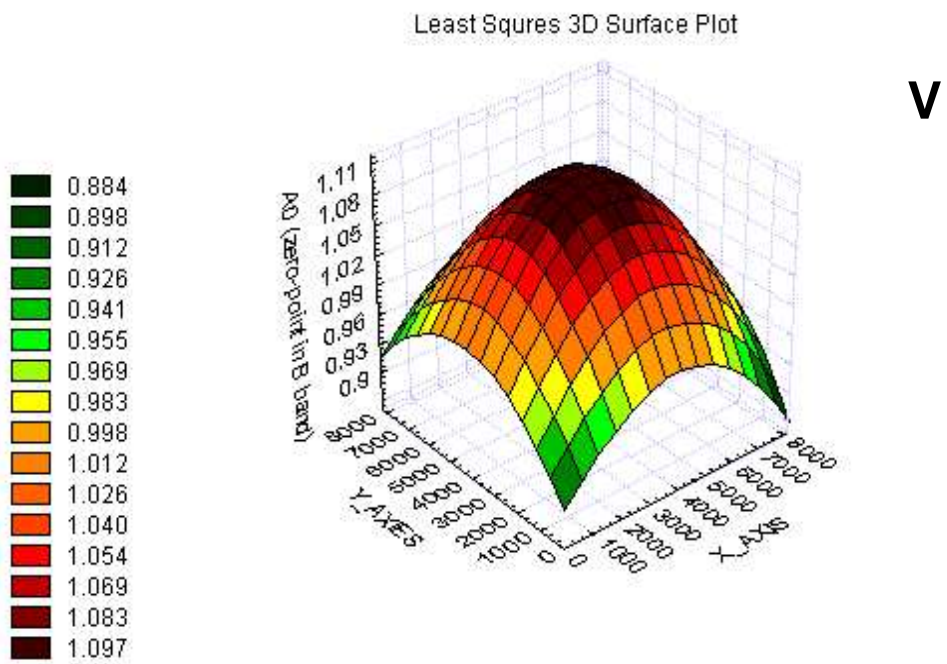
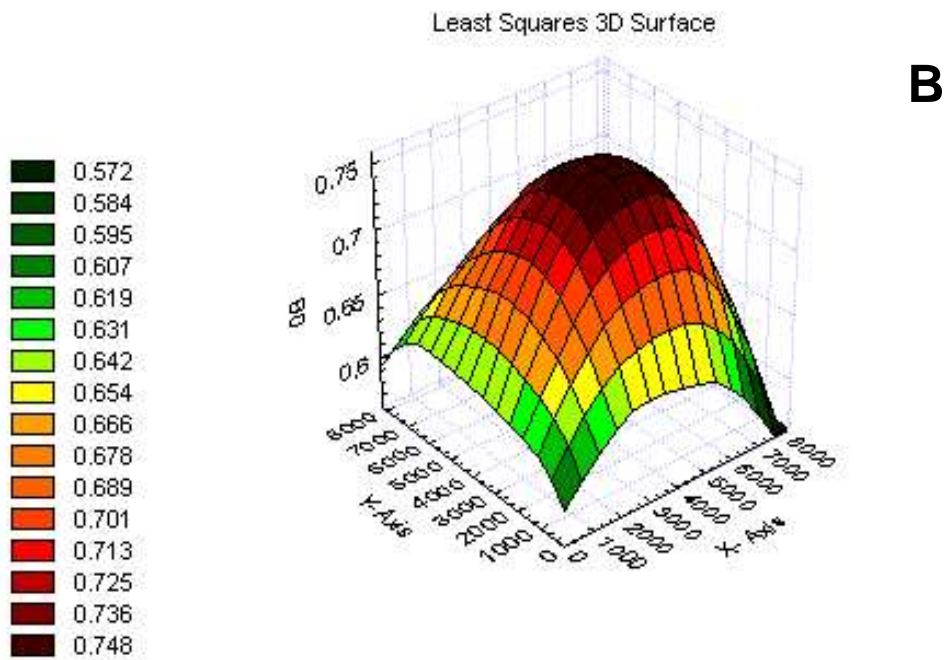


Figure 1: The zeropoint as a function of the X and Y positions in the B and the V bands, as fitted by a 3D least-squares surface. The figure is from Navasardyan et al. [8].

each CCD of the mosaic separately using USNO A2 catalogue entries. The astrometric solution was computed only for the V band, the B, R and I bands are simply matched with the V band images. The astrometric errors are less than 1 arcsecond. An illumination correction has been applied to the data using the assumption that the low-order structure variation seen in the flatfields was the result of illumination variations; a fit was made to this low-order variation and the flatfield was corrected for it. See Sect. 2.3.1 for some more discussion on this topic.

2.3 Data reduction : photometric calibration

The photometry has been done using the packages `daophot` and `daogrow` written by Stetson[12]. The instrumental magnitudes are based entirely on synthetic aperture photometry (bright isolated stars), or profile-fitting photometry with aperture curve-of-growth correction (fainter stars, or those with neighbors less than a few arcseconds away). Star selection is done using parameters like sharpness and roundness of the profile. The zeropoints and color terms were calculated for each CCD of the mosaic using both Landolt and Stetson standard stars. As the data were not sufficient to derive also the extinction correction, the average extinction coefficients k_i adopted were $k_B = 0.22$, $k_V = 0.12$, $k_R = 0.09$, and $k_I = 0.05$.

2.3.1 Illumination correction

It is already known from the work of various authors that, in general, wide field cameras suffer from photometric inhomogeneities. This is also true for the WFI at the ESO 2.2m telescope; Alcalá et al. [1] stress the photometric inhomogeneity among different CCDs. Accurate photometry requires that these inhomogeneities are characterized and corrected for.

The photometric inhomogeneity is unfortunately not a simple offset among CCDs; a significant photometric gradient is evident even across one single chip (Manfroid et al. [7], Koch et al. [5]). This non-uniform illumination is usually attributed to an additional light-pattern caused by internal reflections off the telescope corrector which cannot be corrected by the standard flat-fielding procedures. In order to correct for the effect, one must know the spatial distribution of this pattern. Manfroid et al. [7] describe some strategies for dealing with these calibration errors, but these require special observations. The correction coefficients provided by Koch et al. [5] are only for the V and R bands.

For studying the photometric inhomogeneity across the mosaic area in this work, Landolt[6] standard stars have been combined from SA98, SA101 and Rubin 149. In order to enlarge the set of standard stars for SA98 also Stetson standards have been included². Assuming that the color term is constant over the whole mosaic area and using the averaged value over all the chips, the zero points have been calculated for each standard star. Only brighter stars (those with magnitude less than 15) are used for this purpose. Least-squares 3D surfaces have been fit for the V and B filters. The results are shown in Fig. 1. Both fits show that there is a radial structure.

2.4 WFI results

Standard star catalogs have been extracted from the data for SA110 and for NGC5904. Excerpts from both these catalogs are given in Tables 7 and 8. The complete catalog for NGC5904 lists 4614 stars, and for SA110 3506 stars. A comparison between our magnitude estimates and the magnitudes from the Stetson stars that were included in our catalogs is shown in Figs. 2 and 3. While the results for the NGC5904 field appears to be acceptable, the dispersion in the SA110 field appears definitely larger than our goal. We believe that this is entirely related to

²*Stetson Photometric Standards*, web site: <http://cadwww.hia.nrc.ca/standards/>

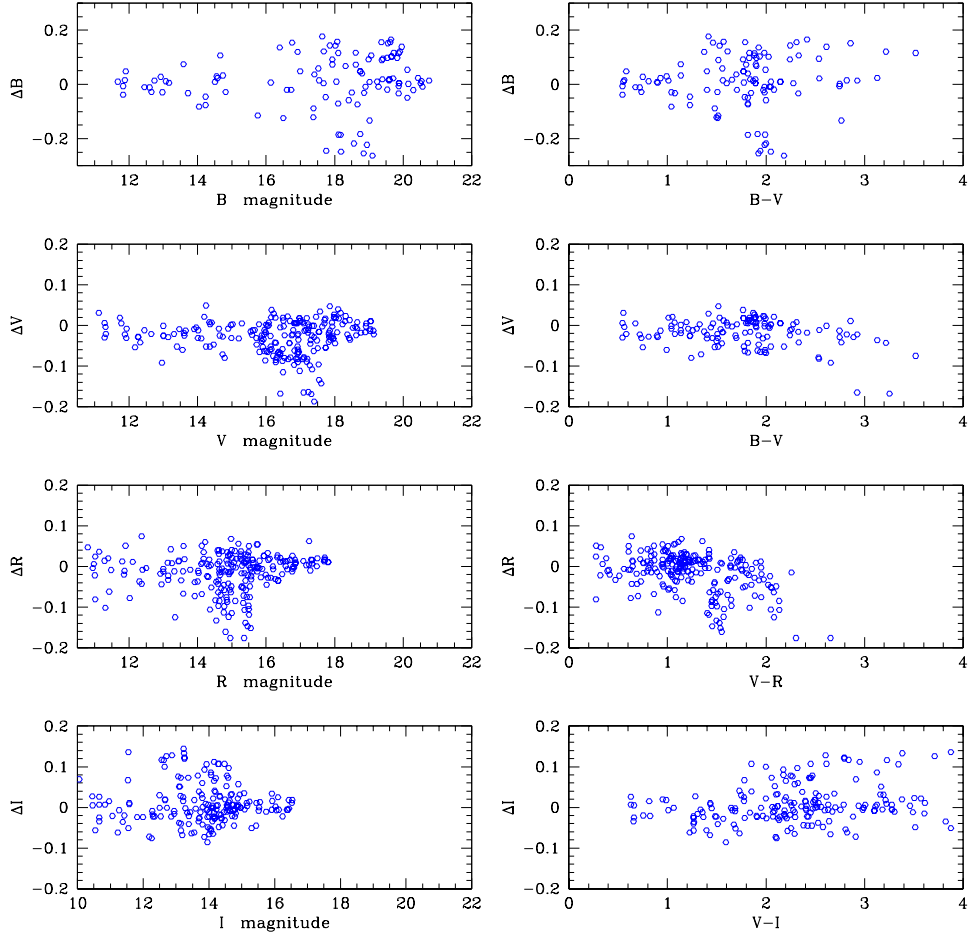


Figure 2: The difference between our photometry of SA110 in the B, V, R, I band-passes and that of Stetson. In each of the panels, the ordinate shows $M_{Stetson} - M_{present\ work}$, and the abscissa $M_{Stetson}$. The figure is from Navasardyan et al. [8].

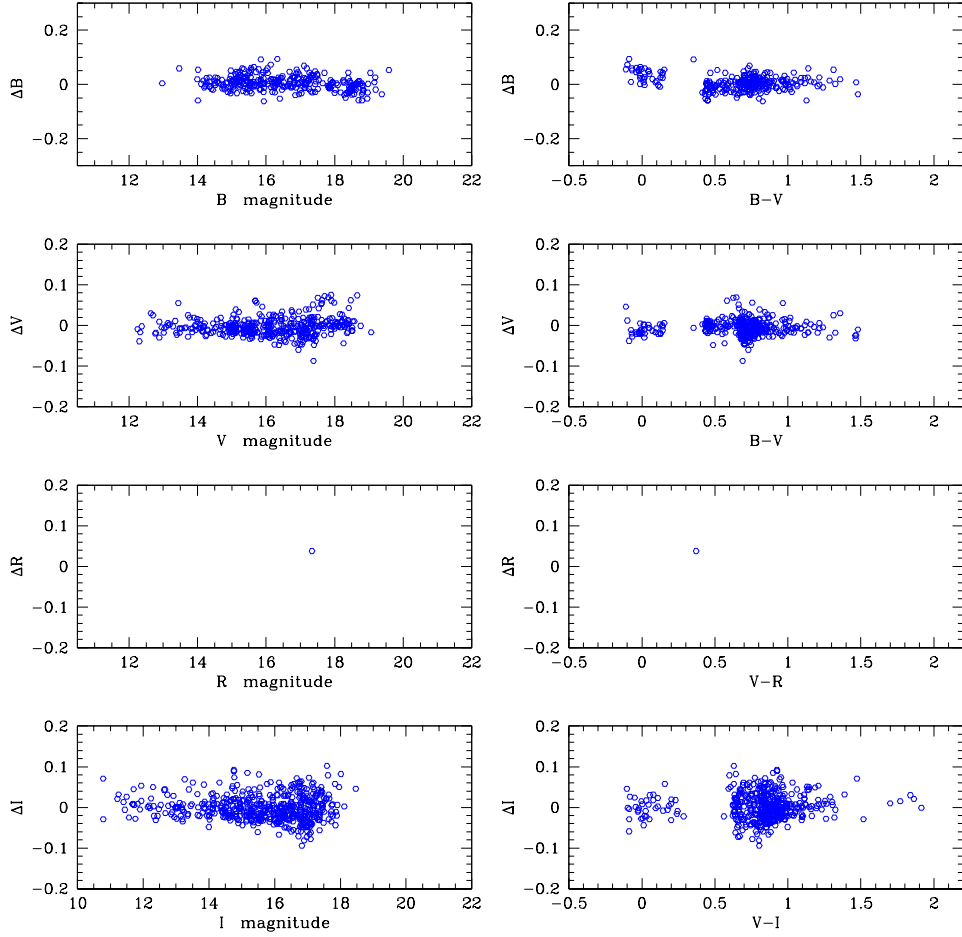


Figure 3: The difference between our photometry of NGC5904 in the B, V, R, I band-passes and that of Stetson. In each of the panels, the ordinate shows $M_{Stetson} - M_{present work}$, and the abscissa $M_{Stetson}$. The figure is from Navasardyan et al. [8].

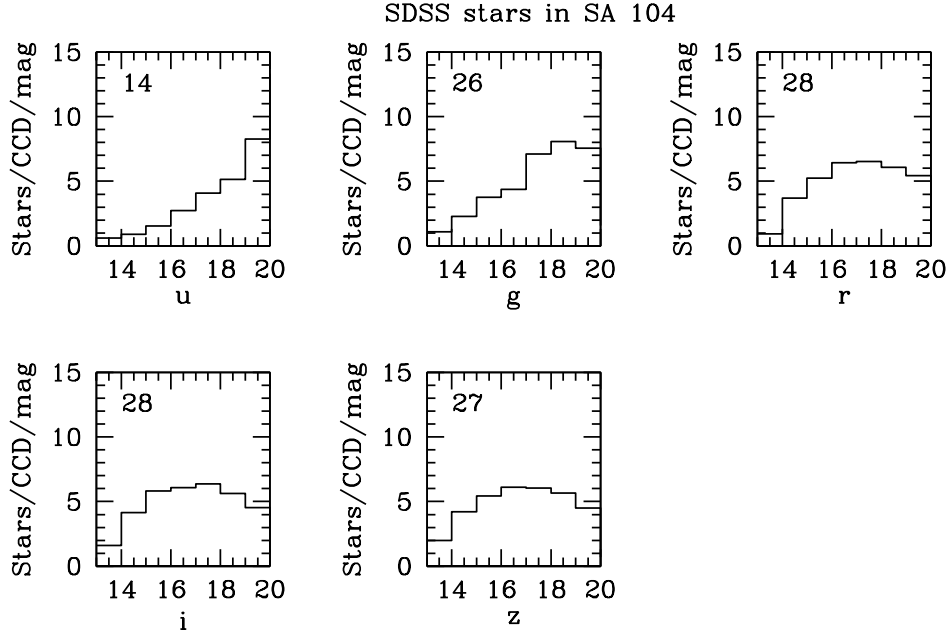


Figure 4: The magnitude distribution of the standard stars in SA104, taken from SDSS Data Release 3. SA104 is the standard field with the highest galactic latitude. The average number of stars per CCD between 14th and 19th magnitude in each filter is printed in each panel.

the limitations of the observational material for SA110. The catalog for SA110 is, therefore, limited in its usefulness.

3 The La Palma - INT/WFC preparatory programme

3.1 Observing runs at the INT/WFC

The La Palma preparatory programme is based on data from three observing runs using the WideField-Camera (WFC) on the 2.5m Isaac Newton Telescope. Like WFI, the WFC is a CCD mosaic camera covering an area of about $0.5^\circ \times 0.5^\circ$, but it uses fewer CCDs than WFI (4) with a larger pixel scale ($0.333''$). The runs were performed in February 2002, June 2002 and February 2003, respectively. The first of these runs suffered from bad weather, and of the total of 15 nights allocated to the programme approximately half were photometric. The Landolt fields observed are given in Table 2. Every Landolt field was observed in a 5-point dither covering $\sim 1.1 \times 1.1$ square degree on the sky. To cover an adequate range of magnitudes, of every pointing both a short (~ 10 s) and a long exposure (~ 300 s) were made. All the observations were done in the u' , g' , r' and i' bands. Of all the equatorial Landolt fields needed for OmegaCAM only SA95 has not been observed. The total volume of raw data generated over the three runs combined is ~ 200 Gb.

Stars between 14th and 19th magnitude can be used for calibration. The equatorial fields have average surface densities of between 20 and 80 such stars per $7.5' \times 15'$ OmegaCAM CCD, depending on the passband and the galactic latitude (see Figure 4).

Table 2: The central pointings used in the La Palma INT observing runs. The level of completion for the data reduction is given in the penultimate column. Fields identified with a * are covered by the SDSS DR3. SA95 could not be observed.

STD FIELD	$\alpha(2000.0)$	$\delta(2000.0)$	l^{II}	b^{II}	Completion	Run
SA 92*	00 55 47	+00 56 57	125	-61	0%	June 2002
SA 98	06 52 05	-00 19 41	213	0	100%	February 2003
SA 101*	09 56 27	-00 23 09	238	40	100%	February 2003
SA 104*	12 42 22	-00 33 09	298	62	100%	February 2003
SA 107*	15 39 35	-00 15 07	6	41	100%	June 2002/Feb 2003
SA 110	18 42 43	+00 20 53	32	2	100%	June 2002
SA 113*	21 42 08	+00 29 36	56	-36	50%	June 2002

3.2 Data reduction

All data has been reduced with the OmegaCAM pipeline. The data reduction consisted of the usual steps of de-biasing, flatfielding and astrometric calibration. The masterflat was constructed from domeflats and twilightflats. For the i' band some fringing was present, but the pattern was not pronounced enough to derive a reliable fringeeflat; no de-fringing has therefore been applied. One issue impacting on the quality of the final reduction that has not been addressed yet is the non-linearity of two of the chips of the INT/WFC (in one case, up to 10%!). This issue is under investigation. The progress made so far in the data reduction of the La Palma data is given in Table 2. Analysis of the measurements continues.

3.3 Color terms

Color terms for the u' , g' , r' and i' bands have been determined for our data. The analysis was based on catalogs derived from the data of all the five pointings in the fields SA101 and SA107 using the secondary standard stars from SDSS DR3. The catalogs were derived using the standard photometric pipeline recipe (**Recipe- PhotCal_Extract_Resulttable** - req. 562), and analyzed interactively.

The color terms were all found to be small or even non-existent. This is not surprising, because the Sloan filters at the INT/WFC closely match the original ones. The color terms for g' and i' are 0.14 ± 0.01 and 0.07 ± 0.01 , respectively, using $(g'-r')$ and $(r'-i')$ as the colors. No evidence for any color term was found for the u' and r' bands. Figure 5 shows some of the data on which the results are based. Further analysis will improve on the uncertainty on the results.

3.4 Illumination correction

No illumination gradients across the detector block of the INT/WFC are known to exist (M. Irwin, private communication). Nevertheless, the possible presence of these gradients has been verified (**Recipe- Illumination_Correction_Verify** - req. 548). These checks are done by plotting the zeropoints of the individual standard stars against their x and y position in the focal plane of the INT/WFC. The verification did not reveal any appreciable illumination variations. The results for the g' band are shown in Fig. 6. The data points from the different chips have been corrected for chip-to-chip differences in the gain, and the color term for the g' band has been applied (see Sect. 3.3). The figure shows that if any illumination variation is present, that it is below 0.03 mag across the whole FoV.

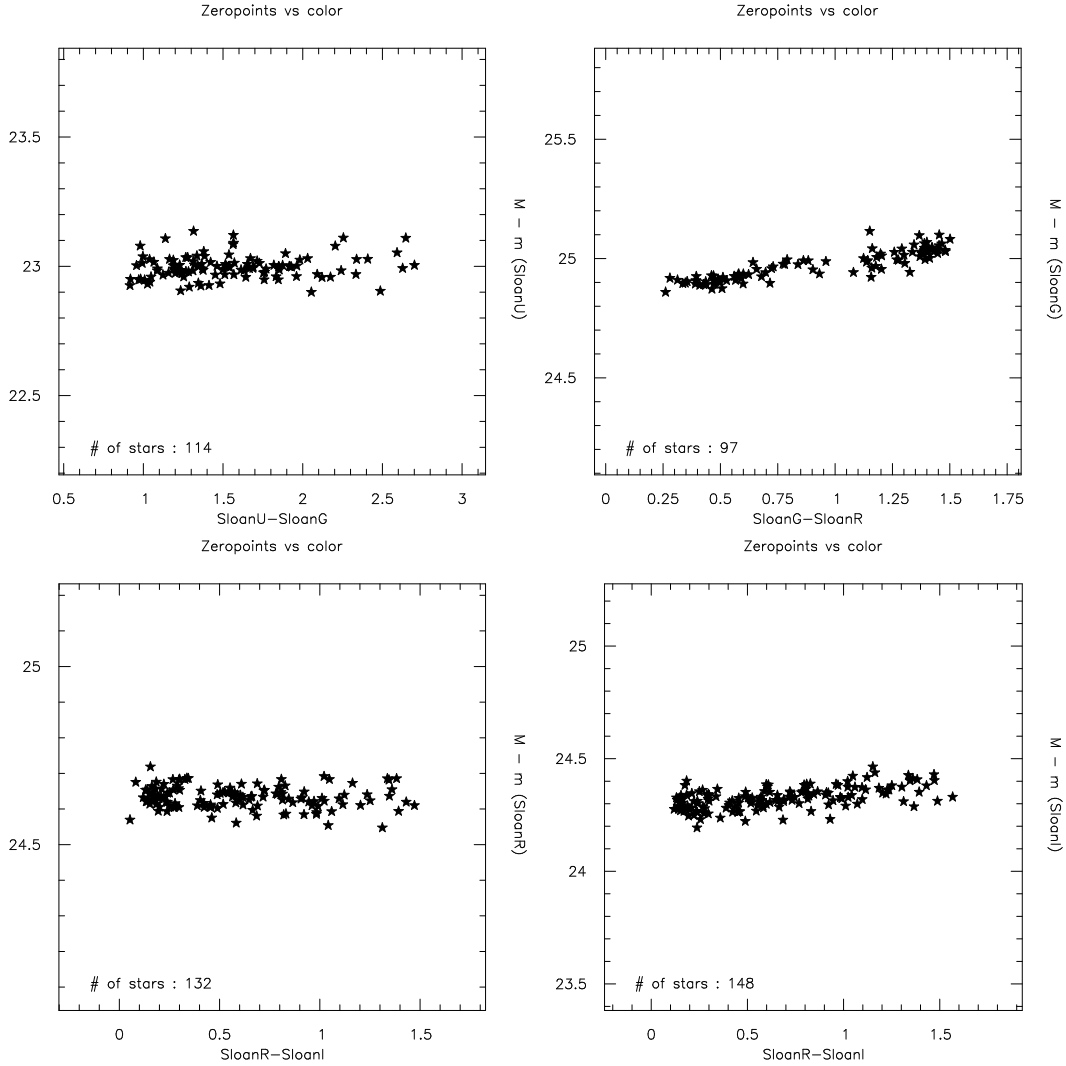


Figure 5: Zero-point-vs-color plots for the u' , g' , r' and i' bands. The data for the standards used in the analysis is obtained from SDSS DR3. In each panel, the x-axis shows the color as catalogued in SDSS DR3, and the y-axis shows the difference between the SDSS DR3 magnitudes of the stars and our measurements.

3.5 Preliminary results - a typical table

Source catalogs have been derived from the data. To give an example of the large quantity of suitable standard stars that can be found on just one chip, a catalog that has been derived for one extension (chip) of the central pointing of SA98 is presented here. The measured fluxes from the stars on this extension were compared with the measured flux of the standard stars 98-1124 and 98-634 also present on this extension. These two standards were put on the Sloan system by applying the transformation equations from Smith et al. [11]. The resulting catalogs contain each ~ 880 candidate sources in the $14 < m < 19$ range. Excerpts of these catalogs are shown in Tables 9 and 10 for the g' and r' bands, respectively.

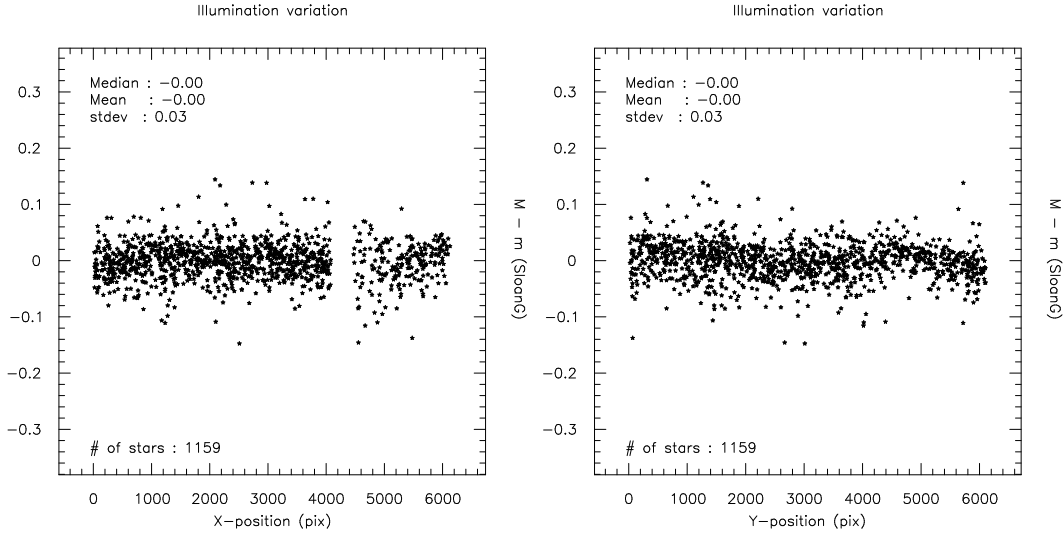


Figure 6: Zeropoint-vs-position plot for the g' band. The data for the standards used in the analysis is obtained from SDSS DR3. In both panels, the x-axis shows the pixel positions of the individual standard stars in the focal plane of INT/WFC. The y-axis shows the difference between the SDSS DR 3 magnitude of a star and the one measured by us. The data points from the different chips have been corrected for chip-to-chip differences in the gain, and the color term for the g' band has been applied to our measurements (see Sect. 3.3).

4 Error budget - error propagation

A break-down of all the sources of error in the OmegaCAM pipeline is presented in Table 3. The table gives the accuracy of the separate steps as required by ESO-DFS (when applicable), and a reference to the relevant requirements as described in Valentijn et al. [10] and Rengelink et al. [9]. Also given in this table is the achieved accuracy. The items in this table are briefly discussed in this section. The photometric part of the pipeline uses fully reduced images as input, so any errors propagating through the image processing part of the pipeline also play a role here. The quality of the photometry is, therefore, a good measure of the quality of the processing system as a whole.

4.1 Flat-fielding

The flatfielding in the OmegaCAM pipeline is done using a master flatfield (**Recipe- Master Flat** - req. 546) that is derived from a suitable combination of master domeflat, master twilight-flat and (if available) master nightskyflat frames. After flatfielding the science data, the flatness of the background should be accurate within 2%.

Tests of the quality of the flat-fielding have been performed on WFI data observed in the U, B, V, R and I bands (Héraudeau[4]). For most of these, the quality of the flat-fielding meets this criterium (especially I). For the U band, the results are inconclusive (see also Table 3).

4.2 Illumination correction

The OmegaCAM system treats the illumination correction as a multi-step process. First, a quick verification is done to ascertain whether illumination variations are actually present (**Recipe-**

Table 3: Summary of sources of error in the OmegaCAM pipeline. The second column gives the accuracy as stated in the requirements (also required by ESO-DFS). The third column gives the achieved accuracy. The entries in the last column refer to the applicable requirements as described in Valentijn et al. [10] and Rengeling et al. [9].

Source of error	Required acc.	Achieved acc.	Note	Ref.
bias	$(\text{RON}/\sqrt{10})^\dagger$	$\sim 0.1\%$	1	req. 541
flat-field	$< 2\%$	$\sim 0.5\%$	2	reqs. 542-547
illumination correction	$< 1\%$	N.A.		req. 548
astrometric calibration	$0.1''$ rms	$0.17''$ rms (α) $0.10''$ rms (δ)		seq. 634
measured standard star magnitudes	< 0.03 mag	≤ 0.02 mag	3	
catalogued standard star magnitudes	< 0.02 mag	~ 0.09 mag	4	req. 569
color terms	$< 2\%$	N.A.		req. 565
atmospheric extinction	$< 5\%$	N.A.		req. 562
zeropoint	$< 5\%$	$\simeq 1\%$	5	reqs. 563-564

\dagger : the accuracy of the master bias is described in terms of the readout noise (RON).

Note 1:

Two master biases, derived from data of two different observations, were divided to get the result. Both were made from 10 raw bias images and the readout noise was 2.0 ADU.

Note 2:

Two master flat fields, derived from data of two different observations, for the same filter and chip were divided to get the result.

Note 3:

Tests of the quality of the aperture photometry are described in Section 5.2. There it was concluded that, for apertures in the range of 3 to 5 times the PSF_FWHM, the difference between MAG_ISO and MAG_APER were less than a few hundreds of a magnitude. The adopted MAG_ISO (and thus the algorithm used to determine the total flux), has internal uncertainties smaller than 0.02 mag.

Note 4:

This number represents the accuracy of the secondary standards at present, not taking into account any color terms or illumination correction (to be determined for La Palma). But see Note 5.

Note 5:

Averaging the zeropoints derived from 20 stars (most CCDs will have at least this many standard stars on them) gives an accuracy improvement of a factor 4.5. Fig. 7 shows that this can be realized: it shows a comparison between the zeropoints derived for 26 Landolt stars on a single CCD. Landolt's magnitudes [6] were transformed to the SDSS system using the color equations of [11], which should be accurate to 0.01 magnitude. The results are shown in the left panel of Fig. 7. No color terms for the WFC filters were applied. The r.m.s. of the set of zeropoints is ~ 0.09 mag, resulting in a mean zeropoint for the CCD determined to an accuracy of 0.02 mag. The three outliers are removed from the input data through σ -clipping. The sigma-clipping removes stars from the sample that have mistakenly been identified as a standard star, or that suffer from irregularities in their aperture photometry (e.g. includes a cosmic ray). The right panel of Fig. 7 shows the same stars plotted against their $g'-r'$ color. The r.m.s. scatter seen in the left panel is clearly dominated by color terms (see also Sect. 3.3). Removing a linear color term results in a scatter of only 0.03 mag (see also Fig. 6), allowing the mean to be determined to better than 0.01 mag.

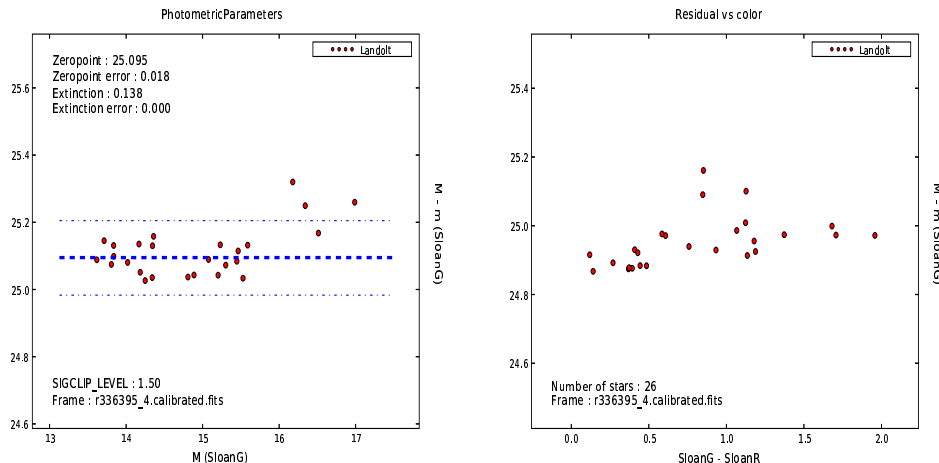


Figure 7: The result of using **Recipe- PhotCal.Extract.Zeropoint** (req. 563) on a single-CCD image observed in the g' band for 26 standard stars from the Landolt [6] catalog (left panel). In the left panel, the x-axis shows the g' magnitudes of the standard stars as derived from their catalogued B and V magnitudes and using the transformation equations of Smith et al. [11]. The right panel shows the same stars plotted against their $g' - r'$ color. Both the g' and r' magnitudes of the standard stars were derived from the catalogued B and V magnitudes using the transformation equations of Smith et al. [11]. In both panels, the y-axis shows the difference between the transformed magnitudes and the ones measured by us.

Illumination_Correction_Verify - req. 548). The results from Sect. 3.4 show that the catalogs produced by the photometric pipeline are accurate enough to do such a quick verification. Second, if any illumination variation is present, it is characterized by fitting the variation of the raw zeropoints of the standard stars as a function of position on the CCD in an interactive analysis (req. 548). This fit is then used to derive an illumination correction frame (**Recipe-Illumination_Correction** - req. 548). This frame is applied to the science data in the image reducing part of the pipeline. The accuracy of the correction to be applied should be good enough to make sure that the ‘photometric flatness’ across the CCD is better than 1% (< 0.01 mag variation in the raw zeropoints across the CCD).

In the case of OmegaCAM, we have the advantage that the focal plane is covered by many CCDs, and of each of these the zeropoint is determined separately and independently. The variation of the illumination across a particular CCD will be a small fraction of the peak-to-peak variation over the full field.

4.2.1 Verifying the presence of illumination variations

The **Illumination_Correction_Verify** recipe creates two sets of products that are used in the verification process: a set of photometric catalogs (the same kind as is produced by **Recipe-PhotCal.Extract.Resulttable**), and a set of zeroth-order illumination correction frames. To show the effectiveness of the recipe, the results of running it on a particular WFI image are shown here. Details of the image used are given in Table 4. The WFI image has been fully reduced with the OmegaCAM pipeline (no illumination correction applied), and the secondary standards used by the recipe were those of SDSS DR3. To derive the R magnitude from the Sloan ones, the transformation equations of Smith et al. [11] were used.

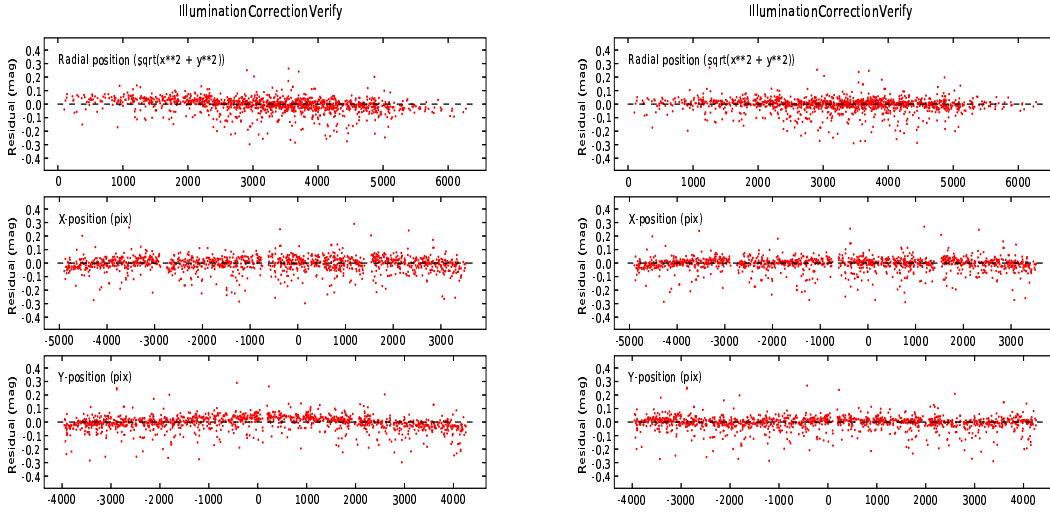


Figure 8: The raw zeropoints of the standard stars on the test WFI image (see Table 4) versus their y-position (bottom), x-position (center) and radial position (top) in the WFI focal plane. The left panel shows the zeropoints *before* applying a rough correction for the illumination variation, the right panel shows the same data *after* applying this correction in the image processing part of the OmegaCAM pipeline. The raw zeropoints from the different chips have been corrected for chip-to-chip differences in the gain. The data for the standards is taken from SDSS DR3. The R magnitudes have been derived from the catalogued g' and r' magnitudes using the transformation equations of Smith et al. [11].

The measured zeropoints of the standard stars on the image as processed by the recipe are plotted in the left panel of Fig. 8 versus their position in the focal plane of WFI. Every single CCD of the image contained approximately 150 suitable standard stars. It is clear from this figure that large variations in the zeropoint across the focal plane do exist. The amplitude and rough shape of the variation in both the x- and y-direction are comparable to those found by Koch et al. [5] (see their Fig. 4).

The illumination correction frames produced by the recipe are shown in Fig. 9 as a multi-extension FITS file. The top-left frame belongs to CCD50, and the bottom-right one to CCD54. The pixel values have linear units so that for image processing purposes the frames can be treated as a flatfield. The pixel values in this image vary from 1.02 in the center to 0.94 in the corners (this corresponds to a variation of 0.08 mag).

To get a feeling for the minimum requirements a given image should meet for the recipe to produce meaningful results several more WFI images were processed by the same recipe. It turned out that in order to get meaningful results, at least 100 or more suitable standard stars should be present on every CCD.

4.2.2 Applying the illumination correction

To show that the OmegaCAM pipeline is capable of applying a correction for illumination variations, the WFI image used in Sect. 4.2.1 has been re-processed by the standard OmegaCAM pipeline using the illumination correction frames displayed in Fig. 9. Photometric catalogs have

then been derived from the image. The measured zeropoints in these catalogs are plotted in the right panel of Fig. 8.

The right panel of this figure shows a clear improvement in the photometric flatness of the image when compared to the left panel. Especially in the y-direction, the variation of the zeropoint has almost vanished and is well below 0.1 magnitude. The scatter in the zeropoints also seems to have been decreased. The case for the x-direction is less clear, but also here a reduction in the scatter is visible. Any residual variation in the zeropoint is possibly due to the ‘rough’ nature of the illumination correction frames that are automatically generated by the `Illumination_Correction_Verify` recipe. A more thorough, interactive characterization of the illumination variation that also takes into account small-scale variations will remedy this.

4.3 Astrometric calibration

The astrometric calibration in the OmegaCAM pipeline is a separate step in the image processing part of the pipeline. The accuracy of the astrometric calibration is required to be better than 0.1'' rms. This is important for accurate co-addition of science data. The photometric part of the pipeline depends on good astrometric calibration to properly identify the photometric standard stars (see Sect. 5.1).

The input reference catalog for the astrometric calibration is the USNO A2.0 catalog of which the sources have a positional accuracy of 0.3'' rms. The results of testing the astrometric calibration with the OmegaCAM pipeline on WFI data are presented in Fig. 10. The tests show that the accuracy of the astrometric calibration is 0.10'' for the declination and 0.17'' for the right ascension. The uncertainty on the astrometric calibration is dominated by the positional accuracy of the sources in the USNO catalog.

4.4 Measuring the standard star magnitudes

Sufficiently accurate aperture photometry on the standard stars in a field is crucial for the quality of the photometric calibration. With a required accuracy of 5% on the overall photometric calibration in the **key bands**, this means that the accuracy on the measured magnitudes should be better than ~ 0.03 mag; this amounts to approximately 97% of the flux inside the aperture or better. In the photometric pipeline, the aperture photometry is delegated to SExtractor[2] (`Recipe- PhotCal_Extract_Resulttable` - req. 562). Some results on testing the performance of the automated aperture photometry are discussed in Sect. 5.2.

4.5 Standard star magnitudes and color terms

The **key band** magnitudes of the stars in the Secondary Standard Star Catalog are required to have an accuracy better than 0.02 magnitude. The required accuracy of the color transformation terms used in the photometric calibration is 2% for the calibration of the **user bands**, and 1% for the transformation between the **key band** monolithic filters and the **composite filter** (req. 565 - to be determined interactively). Color transformations, if needed, are performed on the *catalogued* magnitudes of the standard stars.

4.6 Atmospheric extinction coefficient and zeropoints

The uncertainty on the parameters derived by the photometric part of the pipeline is tied up with all of the errors described in the sections above. The accuracy of the atmospheric extinction coefficient and the zeropoints is required to be better than 5% for the **key bands**. To obtain such an accurate value for both these parameters, a large number of standard stars are needed per CCD (the results plotted in Fig. 6 show that a zeropoint more accurate than 0.01 mag can

Table 4: The WFI image used in the test for the illumination verification.

Image	:	wfi26628
Field observed	:	SA 113
Observing date	:	18 June 1999
Exposure time	:	420 sec
Filter	:	#844 (R)
Airmass	:	1.47

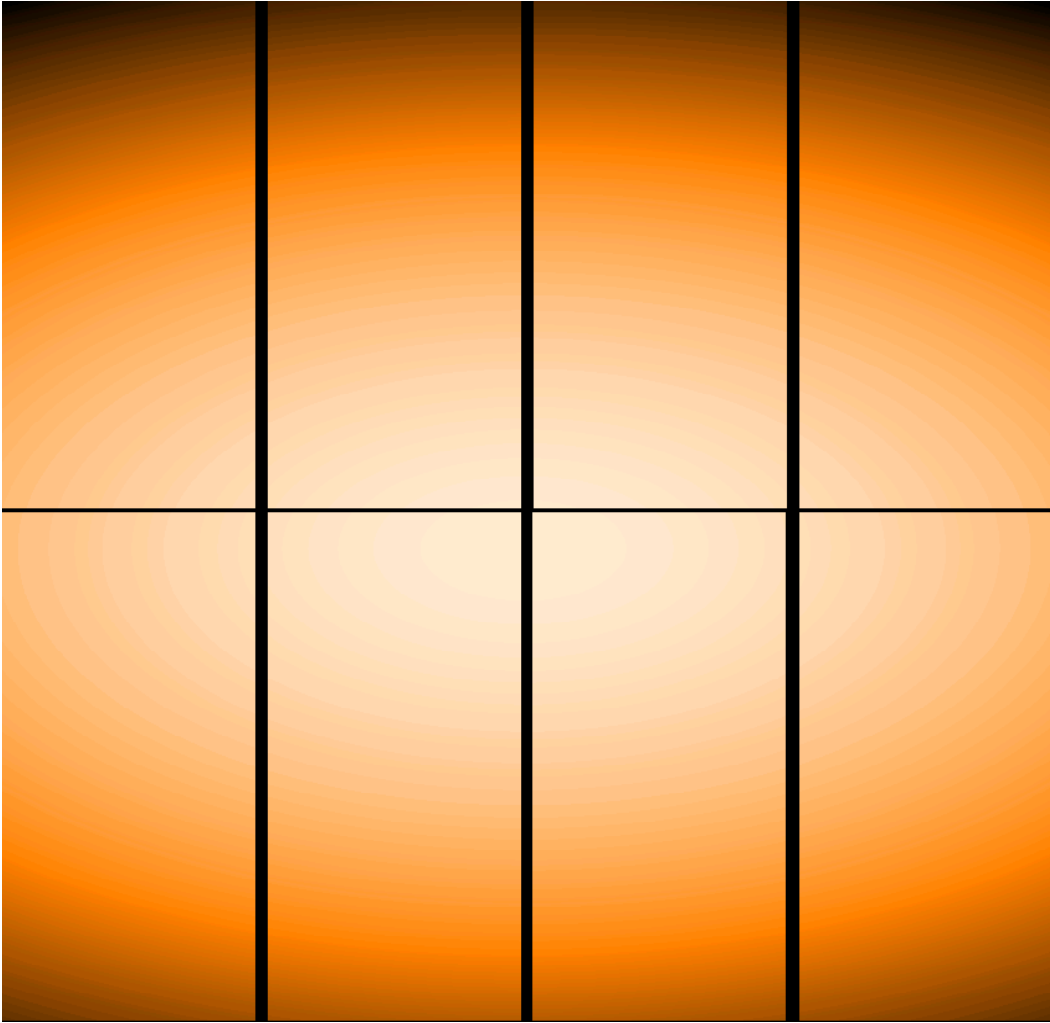


Figure 9: The eight illumination correction frames as produced by **Recipe- Illumination-Correction-Verify** from the test WFI image (Table 4). The pixel values in this image vary from 1.02 in the center to 0.94 in the corners. The top-left frame belongs to CCD50, the bottom-right one to CCD54. The figure was obtained from *skycat* at a scale factor of 1/10.

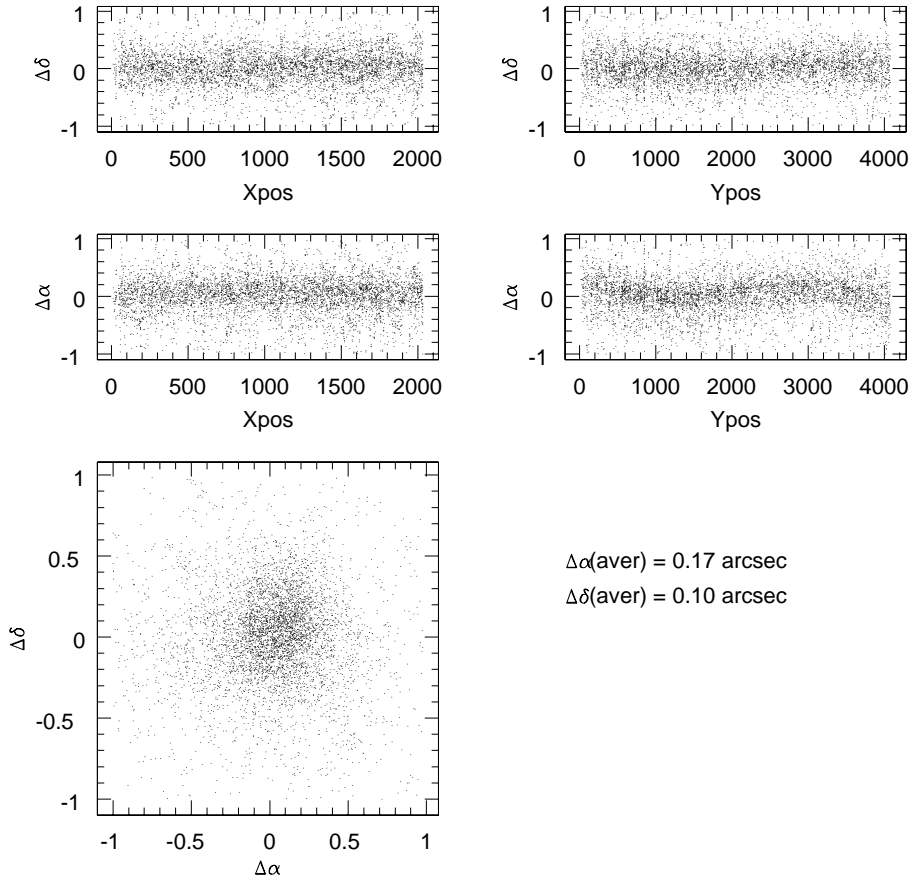


Figure 10: The residuals in the α and δ values after astrometrically calibrating WFI data with the OmegaCAM pipeline. The top panels show the residuals as a function of pixel position on the CCD.

be derived). In Figure 4, the magnitude distribution for the worst-case, highest-latitude field (SA104) is given: in each band there are at least 20 stars per CCD in the 14–19 magnitude range (17 in u').

4.7 Error budget - residuals

The source catalogs for SA98 presented in Tables 9 and 10 contain ~ 20 standard stars from the original Landolt[6] catalog. A comparison between the known magnitudes of these stars, and the values found here (the residuals $\Delta g'$ and $\Delta r'$) provides a handle on the quality of the image processing part of the pipeline. The results of the comparison are shown in Fig. 11. The scatter on the results is ~ 0.06 mag. The only ‘photometric’ sources of this scatter could be the lack of an illumination correction and not taking into account possible color terms. The transformation equations of Smith et al. [11] were used to put the stars from the Landolt [6] catalog on the Sloan system.

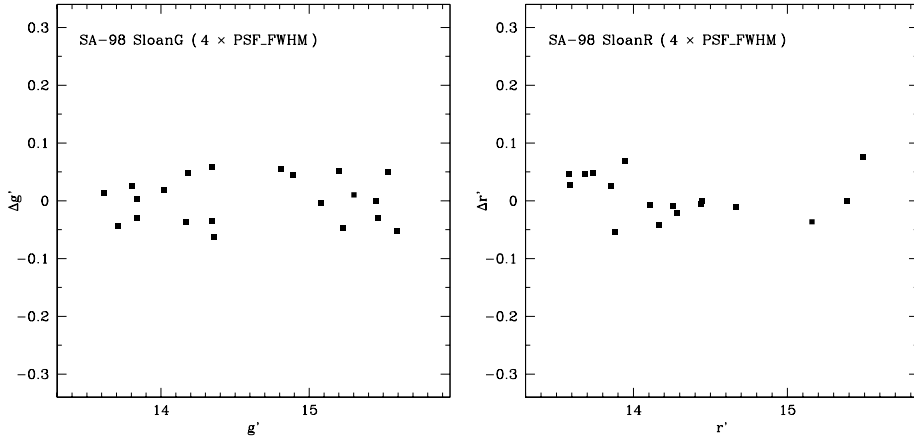


Figure 11: Residual-versus-Sloan magnitudes for the SA 98 catalog given in Tables 9 and 10. The ~ 20 stars from these tables plotted in the figure are standard stars also present in the Landolt [6] catalog. The transformation equations of Smith et al. [11] were used to derive the g' and r' magnitudes from their B and V magnitudes. The x-axis shows these transformed g' and r' magnitudes. The residuals $\Delta g'$ and $\Delta r'$ shown on the y-axis are the difference between the transformed magnitudes of the standard stars and the ones found here. The residuals provide a handle on the quality of the image processing part of the pipeline. The scatter is a (conservative) upper limit on the uncertainty that propagates into the photometric part of the pipeline.

5 Comments on specific software tasks

The photometric software for the OmegaCAM pipeline makes heavy use of source catalogs. These are either catalogs extracted from images of standard fields, or standard star catalogs. The extraction of source catalogs from the input science images is delegated to a dedicated part of the OmegaCAM photometric pipeline (**Recipe- PhotCal_Extract_Resulttable** - req. 562). Two aspects of the catalog extraction that are of particular importance are the robust and correct identification of standard stars, and the quality of the aperture photometry performed on these stars. Both issues will briefly be discussed in this section. Also given is a break-down of the processing time needed for running the full photometric pipeline.

5.1 Standard star identification

Standard star identification is currently done by the *prephotom* tool from LDAC[3]. Although less elaborate than the LDAC *associate* machinery, the performance is found to be good. The robustness of the standard star identification is enhanced by carefully cleaning the source catalogs before association with the standard star catalog. The photometric software removes sources from the catalog that have been flagged by SExtractor[2] as being saturated or having clipped apertures (these sources, therefore, can not negatively influence the further processing in the photometric part of the pipeline). Also removed from the catalog are hot pixels.

The robustness of the standard star identification is found to be high, but some mis-identifications can still occur. However, any mis-identified or multiply identified standard star will clearly show up as an outlier; the *correctly* identified and measured standard stars all have values for the raw zeropoint that cluster tightly around one particular value. Such outliers are removed during processing.

To give an example of the ability of the software to find the standard stars in a given field, catalogs have been derived from a deep exposure of one of the La Palma programme fields using the standard photometric pipeline recipe (**Recipe- PhotCal_Extract_Resulttable** - req. 562). Details of the image used are given in Table 5. Being a deep exposure, the field will be crowded with stars, both standards and *non*-standards. This image, therefore, provides a good test of the robustness of the standard star identification. The image was fully reduced with the OmegaCAM pipeline, and the secondary standards used were those of SDSS DR3.

In this example, approximately 280 standard stars per CCD were identified by **Recipe- PhotCal_Extract_Resulttable**. In Fig.12, the results for the central part of chip A5383-17-7 are shown. The total number of standard stars on this particular chip was 356, of which 283 were found to be *suitable* for photometric purposes. The rejected standard stars were for the most part saturated, or were too close to ‘bleeding’ bright stars.

5.1.1 Standard star identification at high airmass

For the photometric calibration of OmegaCAM, images of the south celestial pole will be taken on a daily basis. As seen from Paranal, the south celestial pole is at a large airmass of ~ 2.40 . It is, therefore, important that the photometric software is capable of finding standard stars at such values of the airmass.

To check the correctness and robustness of the standard star identification on images obtained at high airmasses, catalogs have been derived from one WFI image using the standard photometric pipeline recipe (**Recipe- PhotCal_Extract_Resulttable** - req. 562). Details of the image used are given in Table 6. The airmass of this image (2.30) is comparable with that of the south celestial pole as seen from Paranal. The image was fully reduced with the OmegaCAM pipeline, and the secondary standards used were those of SDSS DR3.

On average, approximately 65 standard stars per CCD were identified as suitable by **Recipe- PhotCal_Extract_Resulttable**. In Fig. 13, the results for the central part of CCD51 are shown. The total number of standard stars on this particular chip was 186, of which 73 were found to be *suitable* for photometric purposes. Many of the rejected standard stars were below the default DETECTION_THRESHOLD used by the recipe (~ 11).

This test shows that it is possible to positively identify enough standard stars for a proper photometric calibration at an airmass comparable to that of the southern celestial pole as seen from Paranal.

5.2 Aperture photometry

The aperture photometry is done in an automated fashion by SExtractor[2]. The default measured magnitude used by the photometric pipeline is MAG_ISO. To check on the validity of the MAG_ISO output of SExtractor when compared with its MAG_APER output, three tests were performed on a fully-reduced single-CCD frame of SA110 from the La Palma preparatory programme. The results are shown in Figure 14. The MAG_ISO values were produced by setting the DETECTION_THRESHOLD configuration parameter for SExtractor on a fixed 5.0 for all three tests. The aperture size used to extract MAG_APER was set at 3.0, 4.0, and 5.0 times the FWHM of the overall fitted PSF model. The PSF model was derived from the frame using PSFEx. Hot pixels, saturated sources, and sources with an ELONGATION > 1.2 were removed from the SExtractor catalog. The total number of legitimate sources plotted in either of the three panels of Figure 14 is approximately 840.

The panels in Fig. 14 show a good agreement between the MAG_ISO and MAG_APER values in the for OmegaCAM relevant range ($14 < m_g' < 19$); the difference between the two is in the order of a few hundreds of a magnitude. However, it is clear from this figure that the ‘correct’ choice of aperture size is very important; too small an aperture and some of the flux of the

Table 5: The INT/WFC image used in the example for standard star identification at deep exposures.

Image	: r336602
Field observed	: SA 107
Observing date	: 11 February 2003
Exposure time	: 300 sec
Filter	: 214 (r')
Airmass	: 1.25

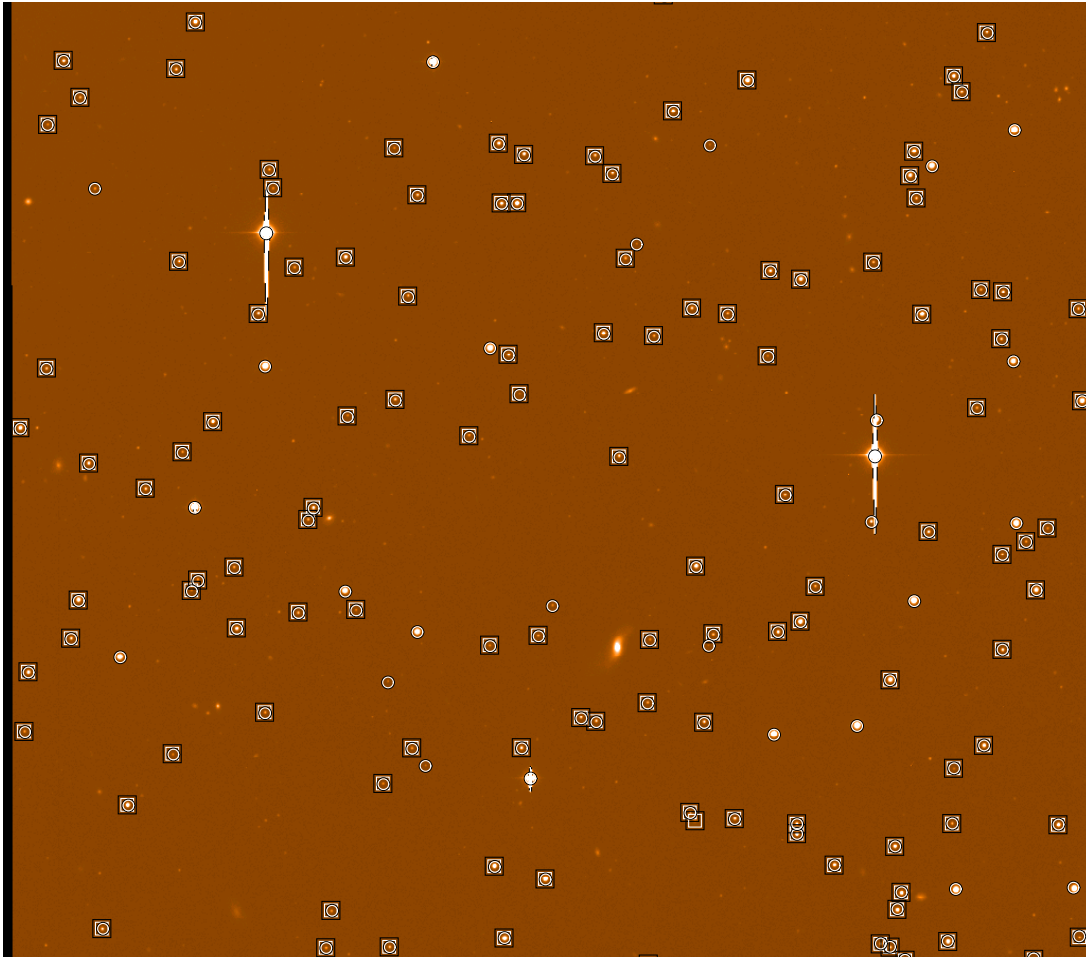


Figure 12: The results from running `Recipe- PhotCal_Extract_Resulttable` on a deep La Palma programme image observed with an exposure time of 300 seconds. Shown is the central part of chip A5383-17-7. The circles denote the sources in the standard star catalog, and the squares show the sources that have been identified by the recipe as suitable standard stars. The secondary standards used are those from SDSS DR3. The figure was obtained from *skycat* at a scale factor of 1/2.

Table 6: The WFI image used in the test for standard star identification at higher airmass.

Image	:	wfi60622
Field observed	:	SA 107
Observing date	:	27 April 2000
Exposure time	:	10 sec
Filter	:	#844 (R)
Airmass	:	2.30

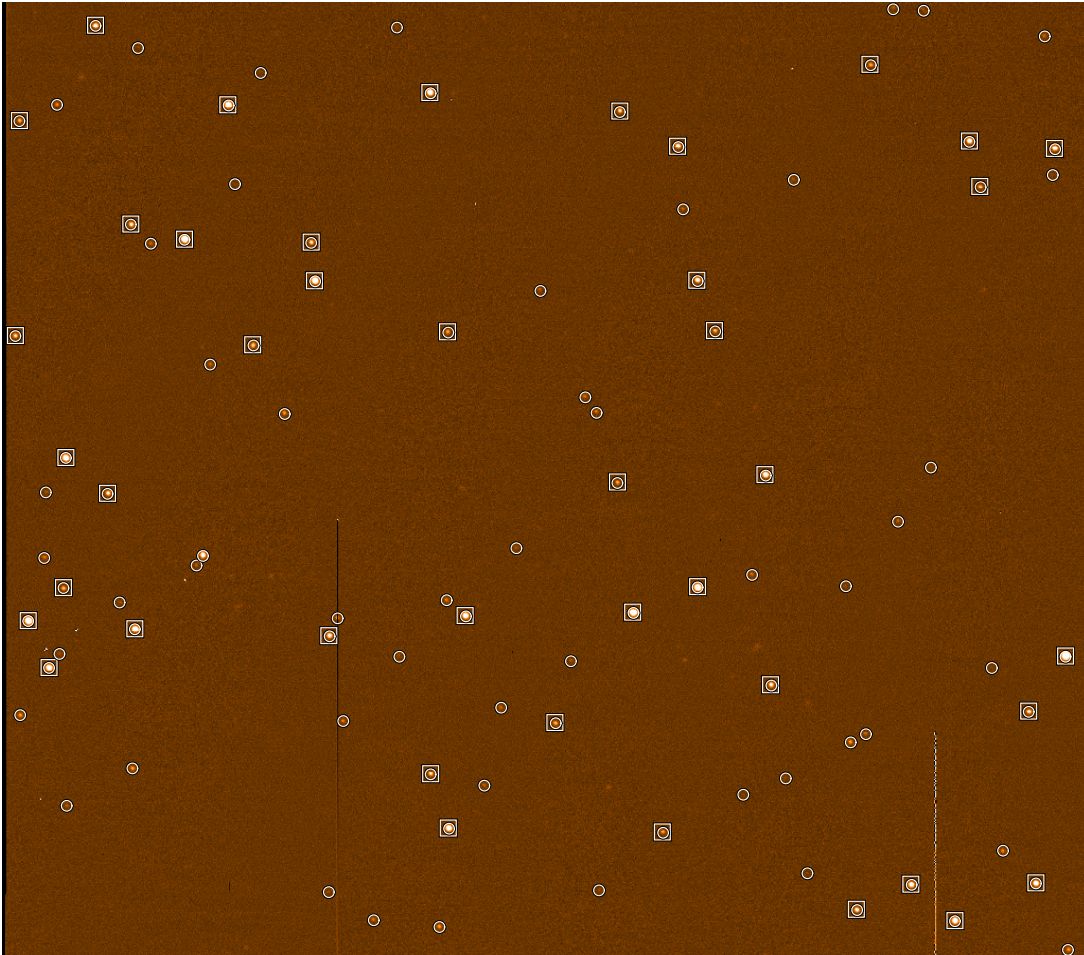


Figure 13: The results from running **Recipe- PhotCal_Extract_Resulttable** on a WFI image observed at airmass 2.3. Shown is the central part of CCD51. The circles denote the sources in the standard star catalog, and the squares show the sources that have been identified by the recipe as suitable standard stars. The secondary standards used are those from SDSS DR3. The figure was obtained from *skycat* at a scale factor of 1/2.

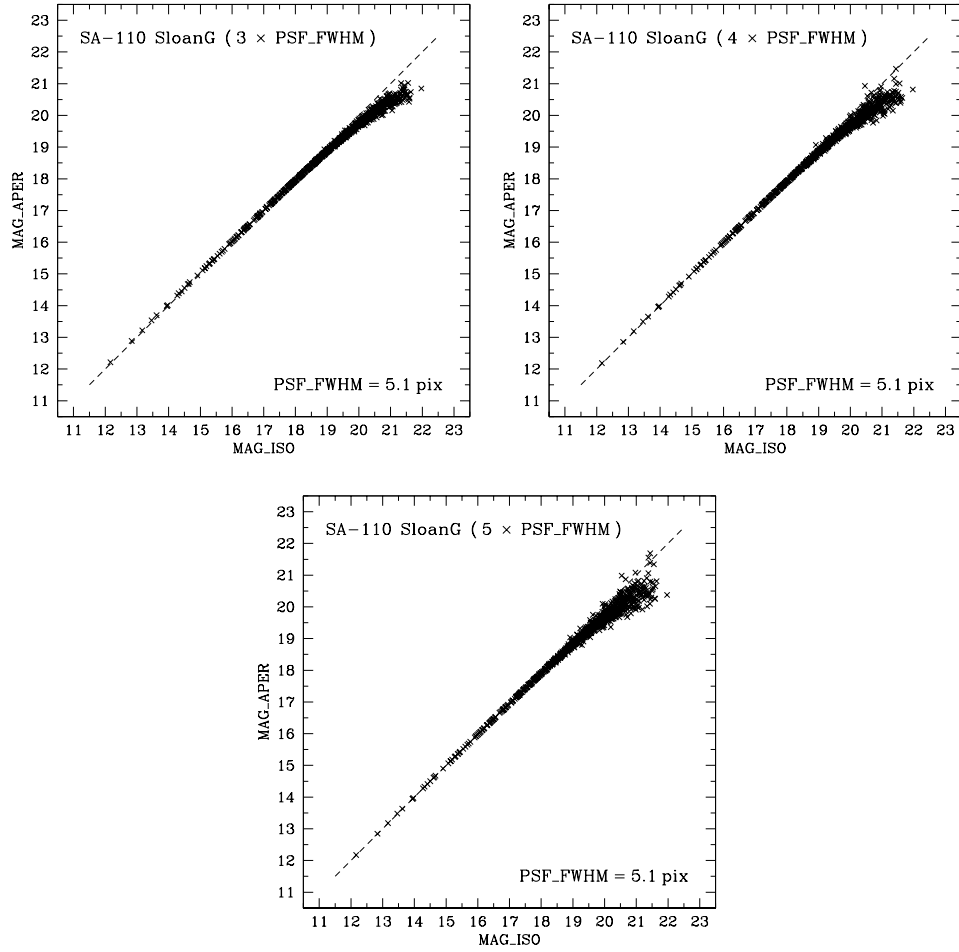


Figure 14: The measured MAG_APER versus MAG_ISO for apertures 3.0, 4.0, and 5.0 times the PSF_FWHM in pixels.

brighter stars will be lost, too large an aperture and the uncertainty on the measured flux will not only increase but will also start to affect the measured fluxes of the brighter stars.

Experience has shown that MAG_APER is the best type of flux to use, because this flux measurement uses a fixed, circular aperture that can be fully controlled through the configuration of SExtractor (and thus be tailored to suit the seeing conditions). The size of this aperture is set by the PHOT_APERTURES SExtractor configuration parameter. The typical aperture used has a diameter of 30-40 pixels which roughly translates to 8"-12".

5.3 Processing time of the photometric pipeline

The time budget for processing the data from the stage of the raw images all the way to the wanted extinction coefficient and zeropoint is divided between the image processing part of the pipeline and the photometric part of the pipeline. The largest part of the total processing time is spend in processing the raw images (de-biasing, flatfielding, astrometric calibration, de-fringing and applying an illumination correction). This process takes ~ 2.5 min for data of a *single* chip. Extracting a source catalog from this chip and associating this with the standard star catalog is found to take ~ 15 secs. This number depends on how crowded the standard field under consideration is, and on the detection threshold limit set for the source extraction software (SExtractor[2]).

The processing time of the catalogs produced from the standard field data depends on the task performed by the photometric part of the pipeline. For deriving the monitoring report (req. 562 in Valentijn et al. [10]), the catalogs from all the pointings of the **standard polar field** must be combined. This will be at least 32×3 catalogs. For deriving the zeropoints (reqs. 563/564 in Valentijn et al. [10]), the 32 catalogs derived from one of the standard equatorial fields are used. The time required for deriving the monitoring report is estimated to be ~ 3 minutes. For deriving the zeropoints for the night, the processing time is ~ 1 minute for one of the **key bands**. The total processing time for the photometric part of the pipeline, therefore, amounts to ~ 7 minutes. Note, that these time estimates are less certain than the ones given in the previous paragraph, because they are mainly based on ‘artificial’ catalogs.

The hardware configuration used in these tests had an Intel P4 1700 MHz CPU and 512 Mb internal memory (see Section 2 of Rengelink et al. [9]). A more detailed breakdown of the estimated processing time can be found in Sections 5 and 6 of Rengelink et al. [9].

6 Summary

Using the results of the La Palma Preparatory programme in particular, we have been able to show that the OmegaCAM DFS pipeline performs to the level needed to allow derivation of photometric zero points with 5% accuracy. Based on real data we have been able to track the errors on photometry that arise from the basis image processing steps (better than 0.5%), and from source magnitude measurements (2%). Comparison with Landolt stars, transformed to the SDSS system (accuracy 1%), shows a scatter of 9%, but this is dominated by a color term in the WFC. Correcting for this term results in an achieved scatter in zeropoint determination from individual standard stars of 3%, which is within the specified 5%. With at least 20 stars per CCD, assuming all errors are random and uncorrelated, this should result in a zero point determination of accuracy around 1%. It is not yet possible to test the size of the errors contributed by the correction for sky concentration, or by color term determinations. We expect these to be dominated by the quality of the calibration data.

Table 7: Excerpt from the standard star list for SA110 as produced by the WFI preparatory programme. The total number of calibrated sources in this list is 3508.

ID	RA	DEC	B	δB	V	δV	R	δR	I	δI
1	18:40:06.8	0:27:40.2	16.579	0.007	15.361	0.009	99.999	9.999	99.999	9.999
2	18:40:07.2	0:29:58.3	21.048	0.040	18.496	0.023	99.999	9.999	15.103	0.013
3	18:40:09.6	0:35:47.4	20.658	0.034	18.450	0.020	17.038	0.014	99.999	9.999
4	18:40:11.5	0:32:54.4	19.418	0.024	17.185	0.011	15.666	0.015	99.999	9.999
5	18:40:12.8	0:27:36.5	15.154	0.009	14.015	0.010	13.218	0.021	12.631	0.019
6	18:40:15.4	0:29:15.2	21.326	0.047	18.875	0.035	17.105	0.018	15.584	0.018
7	18:40:15.9	0:22:40.2	20.432	0.020	18.543	0.035	17.445	0.017	16.094	0.013
8	18:40:16.6	0:25:17.8	15.687	0.036	14.683	0.011	13.986	0.021	13.378	0.018
9	18:40:17.4	0:32:54.6	20.747	0.041	17.622	0.017	15.556	0.016	99.999	9.999
10	18:40:18.7	0:35:47.3	99.999	9.999	18.925	0.029	17.513	0.006	99.999	9.999
11	18:40:18.8	0:24:40.2	15.805	0.012	14.709	0.011	14.022	0.021	13.400	0.018
12	18:40:20.5	0:32:34.1	21.272	0.030	18.548	0.019	16.667	0.016	14.997	0.012
13	18:40:20.8	0:32:59.3	20.308	0.016	18.033	0.015	16.418	0.016	14.987	0.013
14	18:40:21.9	0:24:21.7	21.296	0.045	18.842	0.024	17.134	0.017	15.594	0.013
15	18:40:21.9	0:32:30.8	21.655	0.049	18.502	0.019	16.371	0.016	99.999	9.999
16	18:40:22.2	0:24:50.6	21.619	0.030	17.975	0.014	15.661	0.015	99.999	9.999
17	18:40:26.8	0:26:39.8	20.648	0.018	17.333	0.011	15.148	0.016	99.999	9.999
18	18:40:27.0	0:26:06.1	16.502	0.008	14.928	0.010	13.869	0.022	12.607	0.019
19	18:40:27.3	0:33:34.9	21.566	0.033	18.126	0.015	15.834	0.016	99.999	9.999
20	18:40:27.4	0:33:49.4	19.603	0.015	17.287	0.010	15.758	0.022	99.999	9.999
21	18:40:27.6	0:25:51.1	20.819	0.028	18.323	0.018	16.577	0.017	15.009	0.012
22	18:40:27.7	0:25:40.1	13.296	0.005	12.241	0.009	11.619	0.022	10.962	0.018
23	18:40:28.0	0:34:00.0	21.274	0.040	18.135	0.016	16.032	0.022	99.999	9.999
24	18:40:28.6	0:36:33.8	20.576	0.030	18.142	0.026	16.593	0.005	99.999	9.999
25	18:40:29.4	0:36:06.7	20.614	0.045	18.621	0.041	17.262	0.007	99.999	9.999
26	18:40:29.9	0:21:42.9	21.231	0.029	18.569	0.019	16.856	0.016	15.219	0.019
27	18:40:30.5	0:21:02.6	21.030	0.049	18.705	0.025	17.172	0.017	15.755	0.018
28	18:40:30.5	0:22:13.4	20.622	0.022	17.641	0.017	15.751	0.018	99.999	9.999
29	18:40:30.7	0:21:49.9	19.356	0.017	17.679	0.014	16.524	0.016	99.999	9.999
30	18:40:30.7	0:23:18.0	19.717	0.018	99.999	9.999	16.113	0.028	99.999	9.999
31	18:40:31.1	0:31:26.1	20.188	0.026	17.833	0.017	16.191	0.016	99.999	9.999
32	18:40:31.5	0:22:29.1	20.103	0.018	17.055	0.011	15.160	0.015	99.999	9.999
33	18:40:34.0	0:41:45.6	20.852	0.049	17.707	0.015	15.693	0.012	14.077	0.022
34	18:40:34.1	0:38:55.7	19.905	0.027	17.114	0.012	15.191	0.012	99.999	9.999
35	18:40:34.3	0:24:47.3	19.341	0.031	17.108	0.015	15.936	0.014	99.999	9.999
36	18:40:34.8	0:24:30.0	20.046	0.034	17.856	0.021	16.659	0.015	15.372	0.017
37	18:40:35.3	0:46:01.2	19.827	0.017	16.719	0.008	14.679	0.008	13.004	0.020
38	18:40:35.4	0:38:13.8	18.528	0.013	17.001	0.009	15.967	0.011	14.659	0.012
39	18:40:35.5	0:21:15.0	15.886	0.020	14.578	0.015	13.755	0.014	12.987	0.026
40	18:40:35.6	0:41:23.9	14.297	0.011	13.308	0.011	12.803	0.012	12.147	0.013
41	18:40:35.8	0:24:47.3	19.271	0.012	17.103	0.011	15.960	0.011	14.677	0.017
42	18:40:36.2	0:22:46.7	19.920	0.019	18.192	0.022	17.175	0.016	15.787	0.018
43	18:40:36.9	0:29:36.1	18.467	0.010	16.900	0.016	15.909	0.010	14.944	0.017
44	18:40:37.1	0:31:15.1	15.510	0.010	14.154	0.013	13.345	0.018	12.517	0.024
45	18:40:37.3	0:23:43.4	18.742	0.011	15.244	0.012	13.269	0.018	11.148	0.024
46	18:40:37.5	0:25:46.5	20.966	0.029	18.499	0.021	17.169	0.011	15.718	0.017
47	18:40:37.9	0:47:32.8	20.243	0.027	18.547	0.017	17.458	0.010	16.235	0.012
48	18:40:38.5	0:43:22.9	19.579	0.037	18.018	0.012	16.973	0.009	15.548	0.012
49	18:40:39.6	0:29:29.8	18.471	0.010	15.795	0.013	14.164	0.020	12.533	0.024
50	18:40:39.6	0:34:33.6	19.550	0.021	16.537	0.010	14.753	0.013	99.999	9.999
51	18:40:40.2	0:36:13.0	18.719	0.013	17.187	0.008	16.136	0.008	15.099	0.012
52	18:40:40.3	0:29:09.0	20.826	0.040	18.241	0.017	16.746	0.011	15.207	0.017
53	18:40:40.4	0:37:34.5	20.010	0.019	17.648	0.010	16.076	0.008	14.749	0.012
54	18:40:40.6	0:25:29.9	20.718	0.025	18.382	0.019	17.150	0.011	15.796	0.017
55	18:40:40.9	0:28:02.1	20.969	0.024	17.632	0.013	15.625	0.010	99.999	9.999
56	18:40:41.2	0:32:24.1	19.726	0.015	18.014	0.015	16.987	0.011	15.767	0.017
57	18:40:41.5	0:30:46.3	19.284	0.012	17.035	0.011	15.762	0.011	99.999	9.999
58	18:40:41.5	0:40:41.8	18.800	0.013	17.078	0.008	15.843	0.008	14.772	0.012
59	18:40:41.6	0:37:04.7	11.659	0.010	10.801	0.010	99.999	9.999	99.999	9.999
60	18:40:41.7	0:42:46.2	20.416	0.024	17.483	0.010	15.264	0.011	99.999	9.999

Table 8: Excerpt from the standard star list for NGC5904 as produced by the WFI preparatory programme. The total number of calibrated sources in this list is 4614.

ID	RA	DEC	B	δB	V	δV	R	δR	I	δI
1	15:16:14.6	2:00:14.0	99.999	9.999	17.238	0.023	16.814	0.017	16.350	0.041
2	15:16:15.0	1:48:56.8	17.204	0.014	16.597	0.028	16.294	0.013	15.932	0.029
3	15:16:15.6	1:56:35.9	18.536	0.014	17.547	0.012	16.892	0.013	16.293	0.036
4	15:16:15.6	1:57:43.8	17.746	0.014	16.724	0.015	16.087	0.008	15.514	0.034
5	15:16:15.8	2:00:52.9	99.999	9.999	99.999	9.999	17.463	0.005	16.896	0.034
6	15:16:16.3	1:42:23.3	18.021	0.003	17.304	0.029	16.929	0.013	16.489	0.030
7	15:16:16.6	1:52:52.7	99.999	9.999	99.999	9.999	99.999	9.999	16.417	0.033
8	15:16:16.6	2:05:06.7	99.999	9.999	99.999	9.999	17.409	0.027	16.963	0.044
9	15:16:17.0	1:39:09.2	16.408	0.009	15.397	0.029	14.916	0.008	14.351	0.031
10	15:16:17.6	1:49:12.4	18.664	0.004	17.714	0.018	17.160	0.011	16.600	0.025
11	15:16:17.8	2:00:57.5	17.027	0.019	16.102	0.012	15.602	0.009	15.108	0.029
12	15:16:18.2	1:43:36.2	16.625	0.010	15.582	0.025	14.991	0.007	14.432	0.026
13	15:16:18.3	1:59:26.2	17.658	0.014	16.923	0.013	16.501	0.009	16.007	0.030
14	15:16:18.3	2:20:29.2	99.999	9.999	99.999	9.999	99.999	9.999	17.095	0.019
15	15:16:18.6	1:50:05.3	16.837	0.010	16.059	0.022	15.621	0.006	15.149	0.023
16	15:16:18.9	1:42:45.6	19.002	0.006	18.129	0.018	17.685	0.003	17.232	0.029
17	15:16:18.9	2:12:59.2	18.204	0.012	17.477	0.018	17.063	0.012	16.700	0.028
18	15:16:18.9	2:29:56.8	16.198	0.018	15.773	0.011	15.412	0.010	15.131	0.029
19	15:16:19.2	1:56:03.6	14.944	0.021	14.274	0.011	13.836	0.007	13.470	0.033
20	15:16:19.3	1:42:57.4	16.517	0.009	15.771	0.027	15.375	0.009	14.977	0.027
21	15:16:19.3	1:55:28.9	16.949	0.019	16.404	0.012	16.025	0.007	15.680	0.029
22	15:16:19.3	2:23:44.0	14.668	0.006	13.977	0.026	13.594	0.004	13.173	0.026
23	15:16:19.5	2:35:09.9	17.105	0.027	16.296	0.019	15.940	0.013	15.903	0.037
24	15:16:19.8	1:51:19.0	18.972	0.006	18.431	0.018	18.099	0.007	17.695	0.027
25	15:16:19.8	2:12:37.5	18.612	0.006	18.024	0.019	17.631	0.005	17.304	0.030
26	15:16:19.8	2:18:39.7	14.212	0.004	13.787	0.026	13.518	0.006	13.276	0.025
27	15:16:19.9	2:30:05.2	16.566	0.018	15.977	0.012	15.578	0.012	15.272	0.029
28	15:16:20.2	1:38:10.5	19.234	0.005	17.985	0.018	17.346	0.017	16.654	0.027
29	15:16:20.3	1:40:27.9	18.168	0.003	16.960	0.024	16.279	0.009	15.640	0.023
30	15:16:20.3	2:36:02.2	99.999	9.999	99.999	9.999	17.476	0.032	17.099	0.048
31	15:16:20.4	2:12:13.4	18.461	0.007	17.791	0.019	17.358	0.014	16.996	0.028
32	15:16:20.5	2:31:00.3	99.999	9.999	99.999	9.999	99.999	9.999	17.237	0.024
33	15:16:20.6	2:01:39.3	99.999	9.999	99.999	9.999	17.306	0.003	16.342	0.023
34	15:16:20.7	1:50:20.0	16.355	0.009	15.714	0.026	15.347	0.008	14.888	0.027
35	15:16:20.7	1:55:12.5	17.843	0.014	17.447	0.016	17.114	0.012	16.831	0.034
36	15:16:20.9	1:41:10.5	19.277	0.006	17.984	0.018	17.297	0.020	16.590	0.027
37	15:16:20.9	2:18:02.8	99.999	9.999	99.999	9.999	99.999	9.999	17.334	0.019
38	15:16:21.0	1:38:34.9	21.385	0.024	20.719	0.029	20.440	0.020	99.999	9.999
39	15:16:21.2	2:30:30.7	17.591	0.014	17.063	0.016	16.681	0.017	16.375	0.032
40	15:16:21.3	1:45:38.3	17.798	0.003	17.288	0.025	16.965	0.011	16.608	0.025
41	15:16:21.6	1:52:40.8	18.419	0.014	17.946	0.008	17.580	0.004	17.208	0.034
42	15:16:21.7	1:56:36.6	99.999	9.999	99.999	9.999	99.999	9.999	17.328	0.024
43	15:16:21.8	2:11:07.7	18.672	0.006	17.857	0.026	17.389	0.018	16.937	0.030
44	15:16:21.9	1:51:30.0	12.665	0.005	11.937	0.025	99.999	9.999	11.306	0.029
45	15:16:21.9	2:03:28.4	17.374	0.022	16.102	0.012	15.342	0.008	14.612	0.029
46	15:16:22.0	1:41:59.8	18.065	0.006	17.512	0.017	17.186	0.011	16.843	0.027
47	15:16:22.0	1:49:26.3	13.788	0.004	12.569	0.024	12.002	0.003	11.364	0.025
48	15:16:22.4	1:48:10.3	13.959	0.004	13.066	0.024	12.630	0.006	12.112	0.025
49	15:16:22.5	1:42:29.5	99.999	9.999	99.999	9.999	99.999	9.999	17.061	0.019
50	15:16:22.5	1:49:37.7	14.820	0.005	14.576	0.025	14.370	0.006	14.152	0.026
51	15:16:22.5	2:29:14.7	18.300	0.014	17.279	0.016	16.528	0.018	15.985	0.030
52	15:16:22.8	1:57:16.0	15.216	0.020	14.391	0.011	13.903	0.009	13.425	0.033
53	15:16:22.9	1:53:27.3	99.999	9.999	99.999	9.999	99.999	9.999	16.858	0.024
54	15:16:23.0	1:54:54.7	17.093	0.019	15.960	0.011	15.203	0.006	14.550	0.028
55	15:16:23.2	2:20:41.0	17.927	0.009	16.803	0.024	16.127	0.012	15.497	0.023
56	15:16:23.5	1:51:31.4	19.146	0.007	18.461	0.018	18.054	0.007	99.999	9.999
57	15:16:23.6	2:14:42.4	16.425	0.014	15.733	0.022	15.357	0.007	15.021	0.023
58	15:16:23.6	2:18:14.6	14.750	0.005	13.868	0.026	13.391	0.004	12.944	0.025
59	15:16:23.9	2:20:43.4	18.780	0.010	18.126	0.019	17.728	0.011	17.352	0.033
60	15:16:24.1	1:59:41.0	17.777	0.014	17.087	0.014	16.660	0.010	16.229	0.031

Table 9: Excerpt from the preliminary standard star list for SA98 as produced by the La Palma preparatory programme. The results shown are those for the g' band ($14 < m_{g'} < 19$). The total number of candidate sources in this list is 880.

ID	RA (deg)	DEC (deg)	g'	$\delta g'$	ID	RA (deg)	DEC (deg)	g'	$\delta g'$
1	103.2038	-0.28448550	16.401	0.046	61	103.1812	-0.26978090	18.897	0.068
2	103.2033	-0.31607590	17.793	0.050	62	103.1786	-0.38325690	16.667	0.047
3	103.2013	-0.28949510	15.499	0.046	63	103.1773	-0.40950880	16.653	0.047
4	103.2033	-0.31707800	18.959	0.070	64	103.1782	-0.25995320	15.387	0.046
5	103.2035	-0.25146700	18.860	0.067	65	103.1786	-0.39463110	18.652	0.062
6	103.2013	-0.36643120	18.106	0.053	66	103.1782	-0.27155320	16.601	0.047
7	103.1985	-0.36916830	14.693	0.046	67	103.1781	-0.37431270	18.524	0.059
8	103.1998	-0.40374560	18.566	0.060	68	103.1748	-0.38470530	14.690	0.046
9	103.1996	-0.42162720	18.144	0.053	69	103.1784	-0.32486670	18.235	0.054
10	103.1977	-0.39257710	16.095	0.046	70	103.1760	-0.37536510	16.371	0.046
11	103.2005	-0.27205190	17.503	0.049	71	103.1781	-0.26702490	17.220	0.048
12	103.1942	-0.41066050	14.514	0.046	72	103.1783	-0.24745000	17.802	0.050
13	103.1962	-0.31838880	15.868	0.046	73	103.1760	-0.30301160	16.690	0.047
14	103.1954	-0.26815300	15.164	0.046	74	103.1766	-0.30873440	16.966	0.047
15	103.1961	-0.33418000	18.665	0.062	75	103.1760	-0.37784690	17.913	0.051
16	103.1932	-0.32835250	15.826	0.046	76	103.1752	-0.36415550	17.327	0.048
17	103.1928	-0.27342610	14.923	0.046	77	103.1746	-0.33380710	16.172	0.046
18	103.1930	-0.40630360	17.725	0.050	78	103.1749	-0.38018660	18.699	0.063
19	103.1928	-0.24642800	15.977	0.046	79	103.1718	-0.36247550	15.261	0.046
20	103.1926	-0.32154020	16.754	0.047	80	103.1739	-0.36008860	17.465	0.049
21	103.1931	-0.33681920	17.501	0.049	81	103.1735	-0.31702460	16.705	0.047
22	103.1933	-0.32408730	17.925	0.051	82	103.1724	-0.41766840	17.714	0.050
23	103.1921	-0.26894250	16.007	0.046	83	103.1737	-0.32869060	18.026	0.052
24	103.1921	-0.27529010	16.937	0.047	84	103.1745	-0.29026280	18.616	0.061
25	103.1921	-0.29914580	17.926	0.051	85	103.1728	-0.24985690	16.607	0.047
26	103.1910	-0.34045350	17.705	0.050	86	103.1731	-0.30895600	18.215	0.054
27	103.1875	-0.38624670	14.470	0.046	87	103.1712	-0.42434780	18.621	0.061
28	103.1899	-0.40937500	18.050	0.052	88	103.1695	-0.27665380	15.158	0.046
29	103.1911	-0.25592810	17.721	0.050	89	103.1703	-0.37393930	17.497	0.049
30	103.1906	-0.31011390	18.156	0.053	90	103.1708	-0.36905760	18.468	0.058
31	103.1888	-0.24327270	16.940	0.047	91	103.1685	-0.34456050	14.574	0.046
32	103.1869	-0.31861840	16.412	0.046	92	103.1688	-0.42534330	16.652	0.047
33	103.1868	-0.39917840	17.728	0.050	93	103.1701	-0.36007030	18.114	0.053
34	103.1877	-0.32026650	17.971	0.052	94	103.1719	-0.24704760	18.870	0.067
35	103.1879	-0.27174180	18.021	0.052	95	103.1709	-0.26807740	18.055	0.052
36	103.1862	-0.30237130	16.945	0.047	96	103.1698	-0.30686230	18.393	0.057
37	103.1863	-0.34347250	18.596	0.060	97	103.1684	-0.41131430	18.789	0.065
38	103.1851	-0.34368480	16.351	0.046	98	103.1679	-0.41330660	18.649	0.061
39	103.1860	-0.29830630	17.753	0.050	99	103.1672	-0.40293970	18.695	0.063
40	103.1849	-0.29456910	16.581	0.047	100	103.1657	-0.27061960	16.665	0.047
41	103.1841	-0.42638900	18.650	0.061	101	103.1635	-0.42003010	18.372	0.056
42	103.1849	-0.33827940	17.909	0.051	102	103.1624	-0.41469710	17.096	0.047
43	103.1830	-0.38698930	16.486	0.046	103	103.1626	-0.42291800	18.689	0.062
44	103.1832	-0.39177660	18.280	0.055	104	103.1608	-0.42023340	15.745	0.046
45	103.1836	-0.36252940	18.765	0.064	105	103.1612	-0.35510960	16.405	0.046
46	103.1834	-0.35197290	18.671	0.062	106	103.1641	-0.24232070	18.566	0.060
47	103.1828	-0.30540680	16.921	0.047	107	103.1616	-0.36953730	18.725	0.063
48	103.1821	-0.39457240	18.043	0.052	108	103.1598	-0.33117640	16.285	0.046
49	103.1832	-0.29175980	18.569	0.060	109	103.1599	-0.40075870	17.434	0.048
50	103.1794	-0.24346320	14.032	0.046	110	103.1600	-0.41108380	17.951	0.051
51	103.1819	-0.36496820	18.209	0.054	111	103.1602	-0.40638600	18.640	0.061
52	103.1827	-0.28152590	18.802	0.065	112	103.1603	-0.36011020	18.000	0.052
53	103.1792	-0.35857360	15.128	0.046	113	103.1597	-0.40275480	18.631	0.061
54	103.1800	-0.37249050	16.156	0.046	114	103.1564	-0.28429640	14.374	0.046
55	103.1799	-0.41313270	17.655	0.049	115	103.1603	-0.27872130	18.788	0.065
56	103.1798	-0.27646400	17.594	0.049	116	103.1595	-0.29008470	18.015	0.052
57	103.1779	-0.30043060	14.783	0.046	117	103.1553	-0.40724190	15.340	0.046
58	103.1793	-0.30255620	16.088	0.046	118	103.1561	-0.38755990	16.096	0.046
59	103.1805	-0.35718880	18.439	0.057	119	103.1574	-0.36146000	17.620	0.049
60	103.1799	-0.35058080	18.417	0.057	120	103.1577	-0.36958520	18.533	0.059

Table 10: Excerpt from the preliminary standard star list for SA98 as produced by the La Palma preparatory programme. The results shown are those for the r' band ($14 < m_{r'} < 19$). The total number of candidate sources in this list is 880.

ID	RA (deg)	DEC (deg)	r'	$\delta r'$	ID	RA (deg)	DEC (deg)	r'	$\delta r'$
1	103.2046	-0.41366900	18.986	0.089	61	103.1849	-0.33827900	17.022	0.059
2	103.2038	-0.28447110	15.483	0.057	62	103.1830	-0.38699380	15.782	0.057
3	103.2039	-0.40050030	18.535	0.074	63	103.1832	-0.39178530	16.963	0.059
4	103.2042	-0.33114100	18.216	0.067	64	103.1840	-0.37561550	18.937	0.087
5	103.2037	-0.35169890	18.973	0.088	65	103.1836	-0.36250450	17.933	0.064
6	103.2046	-0.25020830	18.868	0.084	66	103.1834	-0.35196340	17.880	0.063
7	103.2013	-0.28949030	14.923	0.057	67	103.1828	-0.30540470	16.102	0.058
8	103.2035	-0.25143940	17.527	0.061	68	103.1821	-0.39457050	16.803	0.058
9	103.2032	-0.29322030	18.570	0.074	69	103.1832	-0.34822040	18.374	0.070
10	103.2023	-0.35324700	18.321	0.069	70	103.1832	-0.29175110	17.626	0.061
11	103.1985	-0.36916870	14.076	0.057	71	103.1819	-0.36495260	17.517	0.061
12	103.2011	-0.40250700	18.486	0.072	72	103.1792	-0.35856450	14.607	0.057
13	103.2013	-0.36642350	17.401	0.060	73	103.1827	-0.28152570	17.810	0.063
14	103.2021	-0.27369750	18.250	0.068	74	103.1800	-0.37248370	15.472	0.057
15	103.1996	-0.42163460	17.200	0.059	75	103.1799	-0.41314300	16.757	0.058
16	103.1998	-0.40375810	17.382	0.060	76	103.1810	-0.36334940	18.389	0.070
17	103.2005	-0.27203940	16.747	0.058	77	103.1794	-0.30255590	15.429	0.057
18	103.1978	-0.39258880	15.521	0.057	78	103.1805	-0.35718680	17.677	0.062
19	103.1993	-0.33611410	18.726	0.079	79	103.1799	-0.35056780	17.534	0.061
20	103.1983	-0.39729690	18.962	0.088	80	103.1807	-0.32346150	18.138	0.066
21	103.1988	-0.29191900	18.226	0.067	81	103.1812	-0.26975840	17.984	0.064
22	103.1985	-0.32366600	18.948	0.087	82	103.1779	-0.30042890	14.268	0.057
23	103.1963	-0.31838090	15.111	0.057	83	103.1786	-0.38325680	15.980	0.057
24	103.1955	-0.26814250	14.698	0.057	84	103.1798	-0.27645570	16.822	0.058
25	103.1964	-0.38419510	18.427	0.071	85	103.1782	-0.25994870	14.863	0.057
26	103.1961	-0.33418720	17.755	0.062	86	103.1773	-0.40952090	16.185	0.058
27	103.1929	-0.27341240	14.435	0.057	87	103.1791	-0.30884660	18.901	0.085
28	103.1932	-0.32834640	15.208	0.057	88	103.1781	-0.37430320	17.853	0.063
29	103.1930	-0.40630800	17.014	0.059	89	103.1748	-0.38470960	14.176	0.057
30	103.1935	-0.38046390	18.109	0.066	90	103.1782	-0.27154000	15.796	0.057
31	103.1934	-0.32408510	17.142	0.059	91	103.1784	-0.32485950	17.407	0.060
32	103.1931	-0.33682210	16.316	0.058	92	103.1781	-0.26701260	15.739	0.057
33	103.1926	-0.32153840	16.108	0.058	93	103.1761	-0.37535860	15.817	0.057
34	103.1921	-0.26892390	15.270	0.057	94	103.1783	-0.24743130	16.824	0.058
35	103.1921	-0.27528040	16.165	0.058	95	103.1769	-0.40505820	18.651	0.077
36	103.1928	-0.34951230	18.935	0.087	96	103.1760	-0.37784050	16.015	0.057
37	103.1921	-0.29913460	17.102	0.059	97	103.1766	-0.30873050	15.819	0.057
38	103.1910	-0.34045330	16.957	0.059	98	103.1766	-0.38551240	18.531	0.073
39	103.1875	-0.38625560	14.177	0.057	99	103.1760	-0.30301460	15.960	0.057
40	103.1899	-0.40937590	17.267	0.060	100	103.1752	-0.36414180	16.660	0.058
41	103.1879	-0.27172720	17.081	0.059	101	103.1746	-0.33380560	15.740	0.057
42	103.1911	-0.25592000	16.990	0.059	102	103.1749	-0.38019040	17.873	0.063
43	103.1906	-0.31010720	17.362	0.060	103	103.1739	-0.36007930	16.668	0.058
44	103.1887	-0.29794950	16.443	0.058	104	103.1736	-0.31701280	15.717	0.057
45	103.1889	-0.24325520	16.189	0.058	105	103.1740	-0.39525660	18.406	0.071
46	103.1891	-0.29703050	18.021	0.065	106	103.1737	-0.32867720	16.706	0.058
47	103.1868	-0.39917220	16.591	0.058	107	103.1745	-0.29025060	17.677	0.062
48	103.1888	-0.26525720	18.227	0.067	108	103.1750	-0.26058680	18.654	0.077
49	103.1877	-0.32026560	17.033	0.059	109	103.1725	-0.41767360	16.913	0.059
50	103.1869	-0.31861310	15.760	0.057	110	103.1728	-0.24984500	15.158	0.057
51	103.1863	-0.30236460	15.413	0.057	111	103.1731	-0.30894640	16.681	0.058
52	103.1865	-0.34967040	18.493	0.073	112	103.1742	-0.28921130	18.492	0.072
53	103.1874	-0.30977690	18.670	0.077	113	103.1732	-0.33898680	18.533	0.073
54	103.1851	-0.34368200	15.676	0.057	114	103.1712	-0.42436860	17.814	0.063
55	103.1849	-0.29456820	15.965	0.057	115	103.1735	-0.24142670	18.387	0.070
56	103.1863	-0.34345840	18.048	0.065	116	103.1723	-0.30439930	18.044	0.065
57	103.1860	-0.29829980	16.963	0.059	117	103.1697	-0.34339440	18.350	0.070
58	103.1862	-0.30580880	18.373	0.070	118	103.1685	-0.34456290	14.107	0.057
59	103.1842	-0.42639630	17.871	0.063	119	103.1703	-0.37393610	16.713	0.058
60	103.1865	-0.24697320	18.303	0.069	120	103.1708	-0.36904830	17.691	0.062

Table 11: Cross-references between relevant RIX items from VST-TRE-ESO-23100-0033 Issue 1.0 and the sections in this document where these are discussed.

RIX	Description	Reference
28	Execution time pipeline	Section 5.3
29	Error budget breakdown	Section 4 and subsections
39	Aperture photometry	Section 4.4, Section 5.2
132	Standard star distribution	Section 4.6
144	Aperture photometry	Section 4.4, Section 5.2
147	Standard star distribution	Section 4.6

A Cross-reference table

Table 11 gives cross-references between the for this report relevant RIX items from VST-TRE-ESO-23100-0033 Issue 1.0 (*OmegaCAM Data Flow Software - Preliminary Acceptance Europe Conclusions of the Board*), and the various sections in this document.

B Glossary

This glossary explains the OmegaCAM specific terms used throughout the text.

Standard polar field : standard field centered at the south celestial pole.

Composite filter : filter divided into four kwadrants, one for each **key band**.

Key bands : the four Sloan bands in which OmegaCAM will be maintained continuously. These are the u' , g' , r' and i' bands.

User bands : any other band than one of the **key bands**.

Acknowledgements

We would like to thank H. Navasardyan for kindly providing us with her results on the WFI preparatory programme.

References

- [1] Alcalá, J.M., Radovich, M., Silvotti, R. et al. 2002, SPIE, 4836, 406
- [2] Bertin, E., Arnouts, S. 1996, A&AS, 117, 393
- [3] Deul, E. *Pipeline documentation* Version 1.4 (<ftp://www.strw.leidenuniv.nl/pub/ldac/software/>)
- [4] Héraudeau, Ph. *Study of the flat-fielding of WFI data with ASTROWISE part 1* (<http://www.astro-wise.org/> under *Documents*)
- [5] Koch, A., Odenkirchen, M., Grebel, E.K., Caldwell, J.A.R. 2004, AN, 325(4), 299
- [6] Landolt, A.U. 1992, AJ, 104(1), 340
- [7] Manfroid, J., Selman, F., Jones, H. 2001, *ESO Messenger*, 104, 16

- [8] Navasardyan, H., Cappellaro, E., Piotto, G., Harutyunyan, A. *The preparatory program for the photometric calibration of OmegaCAM* (unpublished)
- [9] Rengelink, R., Boxhoorn, D., Deul, E. et al. 2004 *OmegaCAM Data Flow System - Users and programmers manual* Version 2.11 (VST-PLA-OCM-23100-3126)
- [10] Valentijn, E.A., Begeman, K.G., Boxhoorn, D. et al. 2004 *OmegaCAM Data Flow System - Calibration Plan* Version 2.11 (VST-PLA-OCM-23100-3090)
- [11] Smith, J.A., Tucker, D.L., Kent, S. et al. 2002, *AJ*, 123, 2121
- [12] Stetson, P.B. 1987, *PASP*, 99, 191